*Published online 5 September 2011* *Nucleic Acids Research, 2011, Vol. 39, No. 22* ***9659–9670***
*doi:10.1093/nar/gkr659*

# Identification of novel proteins associated with yeast snR30 small nucleolar RNA

**Vincent Lemay[1], Ahmed Hossain[1], Yvonne N. Osheim[2], Ann L. Beyer[2] and François Dragon[1,*]**

[1]Département des sciences biologiques and Centre de recherche BioMed, Université du Québec à Montréal, Montréal, Québec, H3C 3P8, Canada and [2]Department of Microbiology, University of Virginia Health System, Charlottesville VA 22908-0734, USA

Received August 18, 2010; Revised July 13, 2011; Accepted July 27, 2011

## ABSTRACT

**H/ACA small nucleolar RNPs (snoRNPs) that guide pseudouridylation reactions are comprised of one small nucleolar RNA (snoRNA) and four common proteins (Cbf5, Gar1, Nhp2 and Nop10). Unlike other H/ACA snoRNPs, snR30 is essential for the early processing reactions that lead to the production of 18S ribosomal RNA in the yeast *Saccharomyces cerevisiae*. To determine whether snR30 RNP contains specific proteins that contribute to its unique functional properties, we devised an affinity purification strategy using TAP-tagged Gar1 and an RNA aptamer inserted in snR30 snoRNA to selectively purify the RNP. Northern blotting and pCp labeling experiments showed that S1-tagged snR30 snoRNA can be selectively purified with streptavidin beads. Protein analysis revealed that aptamer-tagged snR30 RNA was associated with the four H/ACA proteins and a number of additional proteins: Nop6, ribosomal proteins S9 and S18 and histones H2B and H4. Using antibodies raised against Nop6 we show that endogenous Nop6 localizes to the nucleolus and that it cosediments with snR30 snoRNA in sucrose density gradients. We demonstrate through primer extension experiments that snR30 snoRNA is required for cleavages at site A0, A1 and A2, and that the absence of Nop6 decreases the efficiency of cleavage at site A2. Finally, electron microscopy analyses of chromatin spreads from cells depleted of snR30 snoRNA show that it is required for SSU processome assembly.**

## INTRODUCTION

Eukaryotic ribosome biogenesis takes place in the nucleolus, a prominent compartment of the nucleus. In the yeast *Saccharomyces cerevisiae*, this process requires around 200 proteins and different small nucleolar RNAs (snoRNAs) to produce functional ribosomes (1). In order to function, snoRNAs associate with specific proteins to form ribonucleoproteins [snoRNPs; (2)]. In *S. cerevisiae*, there are 47 snoRNAs belonging to the box C/D family, and 29 snoRNAs of the box H/ACA class; RRP2, the RNA subunit of RNase MRP, is the sole member of its family (3).

H/ACA snoRNAs act as guides for site-specific pseudouridylation (4,5). They adopt a hairpin–hinge–hairpin–tail structure where box H (ANANNA) is located in the hinge region and box ACA in the tail region, always three nucleotides upstream of the 3′-end (6,7). Boxes H and ACA are important for snoRNA stability and accumulation. The hairpins are generally interrupted by an internal loop, called the pseudouridylation pocket, which contains short sequences complementary to the target RNA that undergoes uridine to pseudouridine (Ψ) isomerization. Box H/ACA snoRNAs also share four common proteins: Cbf5 (named dyskerin in humans), Gar1, Nhp2 and Nop10 (2). Cbf5 is the enzyme responsible for the U to Ψ isomerization [(2) and references therein]. Gar1 is a late assembly protein and it is found only in mature RNPs (8).

Very few snoRNAs are required for the cleavage reactions that remove spacer sequences of pre-ribosomal RNAs (pre-rRNAs). In yeast, box C/D snoRNAs U3 and U14, and box H/ACA snoRNA snR30 are essential for 18S rRNA synthesis (9). RNase MRP is involved in cleavage at site A3, upstream of 5.8S rRNA (10). Processing complexes form co-transcriptionally and can be visualized by electron microscopy (EM) carried out on chromatin spreads of rRNA genes: these complexes appear as granules (or 'terminal knobs') at the 5′-end of nascent rRNA transcripts, forming the so-called 'Christmas trees'. Terminal knob formation and subsequent processing require the U3 snoRNA and all of its associated proteins; the U3 complex binds nascent

*To whom correspondence should be addressed. Tel: +1 514 987 3000 (ext. 2063); Fax: +1 514 987 4647; Email: dragon.francois@uqam.ca

pre-rRNA and is thought to be a major constituent of a small 5′-ETS particle that condenses with pre-rRNA and additional factors to form a larger knob coined the SSU processome (11,12), which is also known as the 90S pre-ribosome (13). In exponentially growing cells, SSU processomes assemble on nascent transcripts almost immediately after transcription of the 18S rRNA, when polymerases have reached just beyond one-third of the rDNA gene. At about two-thirds of the rDNA gene, co-transcriptional cleavage of the RNA [almost certainly at site A2, (12,14)] releases the SSU processome (pre-40S ribosome). There may be subsequent formation of a large subunit knob (LSU processome) at the 5′-end of the remaining transcript (12). In post-logarithmic cells or less favorable conditions, these processing steps are post-transcriptional (12,14).

The snR30 snoRNA is highly conserved from yeast to humans (15). According to secondary structure analyses, snR30 RNA adopts a hairpin–hinge–hairpin–tail structure, and bears the conserved H and ACA motifs [(15); Figure 1A]. Although snR30 snoRNA is associated with the four H/ACA proteins (16–18), it has no known target for pseudouridylation (4,5). However, snR30 snoRNA is essential for the early cleavage steps at sites A0, A1 and A2 that lead to the production of the 18S rRNA of the small ribosomal subunit (15,19). Two motifs identified in the 3′ hairpin of snR30 RNA and its orthologs are important for function (motifs m1 and m2; Figure 1A); mutations in these motifs impair 18S production without affecting snR30 snoRNA accumulation (15). Motifs m1 and m2 base pair with target sequences rm1 and rm2 in ES6, a eukaryote-specific rRNA sequence found in the central domain of the 18S rRNA (20,21). Moreover, additional elements that are essential for 18S rRNA processing were identified in the distal part of the 3′-terminal hairpin of snR30 RNA, suggesting that these elements could be docking site(s) for putative snR30-specific proteins (20).

In this study, we devised an affinity chromatography procedure to purify snR30 snoRNP. We show that snR30 snoRNA is associated with the four H/ACA proteins and a number of additional proteins, including Nop6. We also show that absence of snR30 snoRNA impairs SSU processome assembly and abolishes cleavage at sites A0, A1 and A2. Finally, we confirm that endogenous Nop6 localizes to the nucleolus and that a knockout of Nop6 reduces the efficiency of cleavage at site A2.

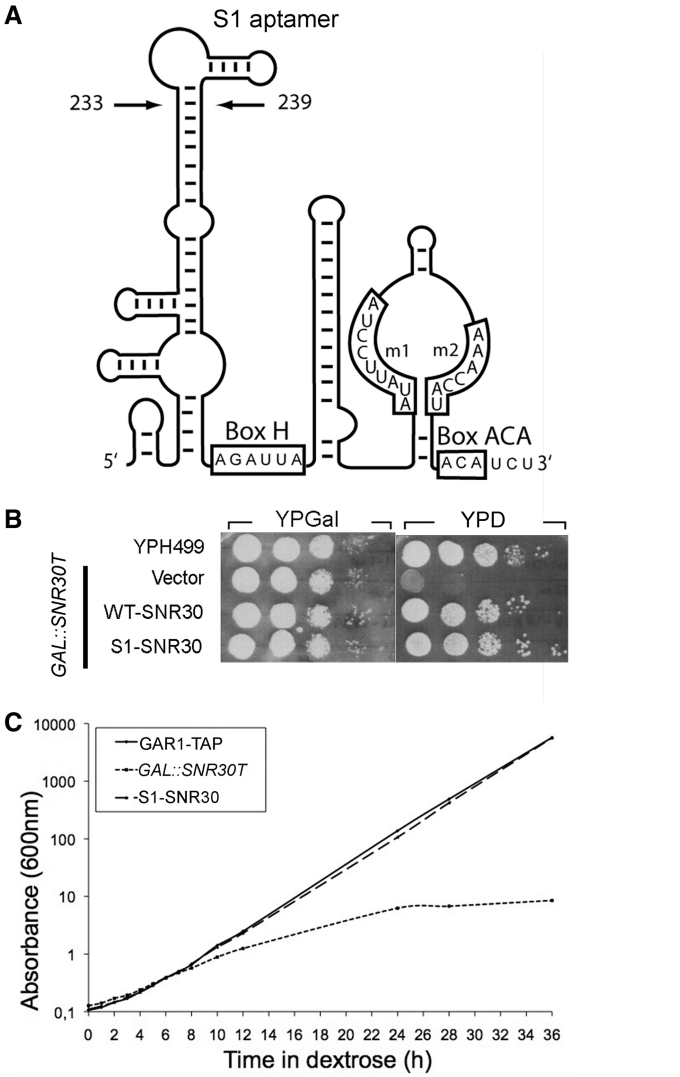


**Figure 1.** S1-tagged snR30 is functional *in vivo*. (**A**) Schematic secondary structure of aptamer-tagged snR30 (not to scale). Box H, box ACA, S1 aptamer, motifs m1 and m2 are indicated. Arrows point to the site where the minimal S1 aptamer was introduced. Residues flanking the S1 aptamer are numbered. (**B**) Ten-fold dilutions of cells were spotted from left to right on YPGal or YPD plates. YPH499 is the parental wild-type strain. Strain *GAL::SNR30T* was transformed with the empty vector pRS316 (Vector), plasmid pRS316-SNR30 encoding untagged snR30 (WT-SNR30) or plasmid pRS316-S1-SNR30 encoding S1-tagged snR30 (S1-SNR30). (**C**) Growth curves of strains GAR1-TAP, *GAL::SNR30T* and S1-SNR30 after shift from YPGal to YPD.

## MATERIALS AND METHODS

### Generation of the S1-snR30 construct

The whole *SNR30* locus, including promoter and terminator sequences [~1.5 kb; (22)], was PCR-amplified from yeast genomic DNA isolated as described (23) and cloned in pBluescript II SK(–). Oligonucleotide sequences are shown in Supplementary Table SI. The minimal S1 aptamer (24) was introduced in the snR30 sequence between nucleotides 234–238 (thus deleting residues 235–237) using the overlap extension method of site-directed mutagenesis (25). The *SNR30* and *S1-SNR30* fragments were cloned in the yeast vector pRS316 (26), to generate plasmids pRS316-SNR30 and pRS316-S1-SNR30, respectively.

### Yeast strains and media

Yeast strains are described in Supplementary Table SII. The strains were grown in rich medium, YPD or YPGal (1% yeast extract, 2% peptone, 2% dextrose or 2% galactose, respectively). When required, strains were grown in SD or SGal (0.67% yeast nitrogen base, 2% dextrose or

2% galactose, respectively) complemented with the appropriate dropout mix, or in the presence of 200 μg/ml G418 (Invitrogen). Yeast transformation was carried out as described (27). Strain GAR1-TAP expressing TAP-tagged Gar1 under the control of its natural promoter was generated as described (28). Strains YPH499 and GAR1-TAP were modified to express snR30 snoRNA under the control of the GAL1 promoter (29); the resulting strains were named *GAL::SNR30* and *GAL::SNR30T*, respectively.

### Spot assays and growth curves

Strains YPH499, *GAL::SNR30T*, *GAL::SNR30V*, WT-SNR30 and S1-SNR30 were grown in galactose-containing medium to exponential phase ($A_{600} \approx 0.5$), harvested, washed and resuspended in sterile water to an OD of 1. Ten-fold serial dilutions of these cell suspensions were spotted onto YPD or YPGal plates that were incubated at 16°C, 30°C or 37°C. For cultures in liquid media, GAR1-TAP, *GAL::SNR30T* and S1-SNR30 strains were grown in galactose-containing medium to exponential phase, harvested, washed with sterile water and resuspended to an OD of 0.1 in YPD pre-warmed at 30°C. During growth in YPD, strains were kept in exponential growth ($A_{600} < 0.7$) by dilution in pre-warmed YPD. For depletion experiments, strains were grown as described above and harvested by centrifugation 9 or 12 h after the shift to YPD.

### Affinity purification of S1-snR30

Cells expressing S1-tagged snR30 snoRNA were grown in YPD to exponential phase ($A_{600} \approx 0.5$) and harvested by centrifugation. The cell pellet was washed twice in ice-cold sterile water and resuspended in TMK150 buffer [25 mM Tris–HCl (pH 7.8), 10 mM $MgCl_2$, 150 mM KCl, 1 mM 1,4-dithiothreitol (DTT), 0.1% NP-40] complemented with Complete protease inhibitor (Roche). The buffer to cell ratio was 10 μl/$A_{600}$ unit. Cells were flash frozen in liquid nitrogen and stored at −80°C. Frozen cells were thawed on ice and whole-cell extract was prepared using 400–625 micron glass beads (Sigma). The lysate was cleared by centrifugation (5 min, 10 000*g*). The cell extract (40 ml) was split into eight tubes and each was incubated with 200 μl of IgG-agarose beads (GE Healthcare) at 4°C for 2 h on a nutator. Beads were placed in eight poly-prep columns (Bio-Rad) and each was washed with 25 ml of TMK150 lacking NP-40 and DTT. Elution from IgG beads was carried out with 1 ml of TMK150-TEV [TMK150 with 100 units of AcTEV protease (Invitrogen) and 60 μg/ml of avidin (Sigma)] for 2 h at 16°C on a nutator. Eluates were pooled and incubated with 400 μl of streptavidin-agarose beads (Sigma) at 4°C for 1 h on a nutator. Streptavidin beads were placed in a poly-prep column, washed with 50 ml of TMK150 and incubated with 800 μl of TMK150 supplemented with 5 mM biotin (Sigma) to elute the S1–snR30 complex. Eluates were split in four samples, two for RNA analyses (3′-end pCp labeling and northern hybridization) and two for protein analyses (western blotting and silver staining).

### RNA analyses

RNAs were recovered by phenol extraction and ethanol precipitation, and labeled at their 3′-end as described (30). Identification of specific RNAs was done by northern hybridization with radiolabeled oligonucleotide probes (11). Primer extension analyses were done essentially as described (31) with primers A0-A1, 18S and A2–A3 (Supplementary Table SI). Dried gels or membranes were exposed to a phosphor screen and revealed with the Molecular Imager F/X$^{TM}$ (Bio-Rad).

### Production of anti-Cbf5 and anti-Nop6 antibodies

The synthetic peptide KEYVPLDNAEQSTSC was used to raise anti-Cbf5 antibodies. Peptide synthesis and immunization were done by Invitrogen. To produce anti-Nop6 antibodies, rabbits were immunized in-house at the Animal Care Facility with recombinant Nop6: *NOP6* ORF was cloned into pGEX-4T-1 and GST-tagged Nop6 was produced in strain Rosetta II (DE3) pLysS (Novagen). GST-Nop6 was purified by affinity chromatography using GSTrap$^{TM}$ columns (GE Healthcare), and recombinant Nop6 was isolated after cleavage with thrombin following recommendations of the supplier. Western blot analyses showed that antibodies raised against Cbf5 and Nop6 specifically recognize proteins of 55 and 25 kDa, respectively (data not shown). For immunofluorescence microscopy (see below), anti-Nop6 antibodies were purified by affinity chromatography with GST-Nop6 coupled to CNBr-activated Sepharose® 4B agarose beads (GE Healthcare).

### Protein analyses

Proteins were separated on 10% SDS–polyacrylamide gels or Criterion XT Bis–Tris 4–12% gradient polyacrylamide gels (Bio-Rad). For western analysis, proteins were transferred onto PVDF membranes (Immobilon-P; Millipore), and immunodetection was carried out with anti-Cbf5 peptide antibodies diluted 1/2000, anti-Nhp2 antibodies (32), anti-Nop6 antibodies diluted 1/1000 or PAP antibody (Sigma). HRP-conjugated secondary antibodies were used according to manufacturer's recommendations (GE Healthcare). Blots were revealed with ECL Plus$^{TM}$ (GE Healthcare). Silver staining was carried out as described (33). Gel slices were analyzed by mass spectrometry (McGill University and Génome Québec Innovation Center, and SAMS Centre for Proteomics at the University of Calgary).

### Validation of mass spectrometry results

Whole-cell extracts were prepared as described above except that 25 $A_{600}$ units of cells were resuspended in 2.5 ml TMK150 buffer. Extracts were pre-cleared by incubation with 50 μl of CL-4B agarose beads (Sigma) at 4°C for 30 min on a nutator. The RNA concentration of each extract was determined by spectrophotometry ($A_{254}$), normalized with TMK150, and 2 ml samples (8 $A_{254}$ U) were incubated with 50 μl of IgG-agarose beads at 4°C for 1 h on a nutator. The beads were washed six times with 1 ml TMK150, resuspended in 100 μl elution buffer

[25 mM Tris–HCl pH 7.5, 10 mM EDTA, 0.5% SDS, 0.1 U/μl RNasin® (Promega)] and incubated at 65°C for 10 min with occasional mixing. RNAs were analyzed as described above.

### Sucrose density gradients

Extracts were fractionated on 7–47% linear sucrose gradients essentially as described (34) except that TMK150 buffer without heparin was used. Sixteen fractions were collected from top to bottom with an ISCO density gradient fractionation system coupled to a UA-6 detector to produce continuous absorbance profiles at 254 nm. Absorbance profiles were used to locate 40S and 60S ribosomal subunits, 80S ribosomes and polysomes.

### Immunofluorescense microscopy

Yeast cells were processed essentially as described (35). Purified anti-Nop6 antibodies and mouse monoclonal anti-fibrillarin antibody 17C12, which recognizes the nucleolar marker fibrillarin and its yeast homolog Nop1 (36), were diluted 1/500 in blocking buffer (0.5% BSA, 0.5% Tween 20 in PBS) and incubated overnight at 4°C. Secondary antibodies Alexa Fluor®488 goat anti-rabbit IgG and Alexa Fluor®555 goat anti-mouse IgG (Invitrogen) were diluted 1/1000 in blocking buffer and incubated for 30 min at room temperature. Nuclear DNA was stained for 15 min with 1 μg/ml of 4′-6-Diamidino-2-phenylindole (DAPI). Coverslips were washed with blocking buffer and slides were mounted with ProLong® Gold antifade reagent (Invitrogen). Specimens were observed with an Eclipse Ti inverted microscope (Nikon) with an apochromat objective (numerical aperture 1.4); images were acquired with a Monochrome CCD camera (CFW1312 from Scion Corporation) and processed with ImageJ V 1.34s (Wayne Rasband, National Institutes of Health, USA).

### Chromatin spreads and electron microscopy

The *GAL::SNR30* strain was used to carry out chromatin spreads essentially as described (11,12). Exponentially growing cells were shifted from YPGal to YPD medium and incubated for 5 h to deplete the snR30 snoRNA. Hundreds of rRNA genes were seen in chromatin spreads from both control and snR30-depleted cells, with representative examples shown in Figure 9. The experiment was repeated with similar results.

## RESULTS

### Affinity purification of snR30 snoRNP

To selectively purify snR30 snoRNP by affinity chromatography and identify its protein components, we designed a two-step purification strategy to be used with a modified yeast strain. The TAP tag (28) was fused to the C-terminus of the H/ACA protein Gar1 (strain GAR1-TAP). It is worth noting that we chose to tag Gar1 because this protein is found only in mature, functional H/ACA RNPs (8). The TAP tag was used to recover the entire family of H/ACA snoRNPs. As there is no known snR30-specific protein that could be used to selectively isolate snR30 snoRNP from the pool of H/ACA snoRNPs, we introduced an RNA tag in snR30 snoRNA (Figure 1A). We used the minimal S1 aptamer, which has high affinity and specificity for streptavidin (24).

Since snR30 snoRNA is essential for viability, sequence modifications that interfere with its function cause cell death (15,22). To test whether the introduction of the S1 aptamer in snR30 snoRNA interferes with its function, strain S1-SNR30 was first grown to logarithmic phase in galactose-containing medium to allow expression of both chromosomally encoded snR30 and plasmid-borne S1-snR30, and then shifted to dextrose-containing medium to turn off the GAL1 promoter (29) and shut down expression of untagged snR30 snoRNA. In the absence of chromosomally encoded snR30 snoRNA, these cells rely solely on plasmid-borne S1-snR30 snoRNA for survival. On YPD plates incubated at 30°C, strain S1-SNR30 grew as well as the wild-type strain YPH499 or the control strain WT-SNR30 expressing untagged snR30 snoRNA from a single-copy plasmid, in marked contrast with the *GAL::SNR30T* strain containing the empty vector pRS316 (Figure 1B). Strains were also incubated at 16°C and 37°C, and no difference in growth was observed (data not shown). We compared growth in liquid medium after shifting strains from galactose- to dextrose-containing medium. The growth rate of strain *GAL::SNR30T* (without plasmid-borne snR30) began to slow down just around 5 h after the shift to YPD, and growth was significantly impaired after 24 h of depletion (Figure 1C). In contrast, the strain expressing S1-snR30 snoRNA grew as well as strain GAR1-TAP in YPD (Figure 1C). These results demonstrate that S1-tagged snR30 is functional.

We used the S1-SNR30 strain grown in YPD for our affinity purification procedure. For affinity selection done in a single step, extracts were incubated with streptavidin–agarose beads to selectively isolate the snR30 complex. Single-step purification of S1-snR30 by streptavidin beads was compared with the immunoprecipitation (IP) of H/ACA snoRNAs by Gar1-TAP. After elution, the RNAs and proteins of the purified RNPs were recovered and analyzed. First, RNAs were extracted and examined by polyacrylamide gel electrophoresis after 3′-end labeling. These experiments revealed RNA bands corresponding to H/ACA snoRNAs associated with Gar1-TAP (Figure 2A, lane 3). A band corresponding to S1-snR30 was enriched when single step streptavidin purification was done (Figure 2A, lane 4). Bands for 5.8S rRNA, 5S rRNA and tRNAs could also be detected but these are normal contaminants of 3′-end labeling (11,37). In order to specifically identify snoRNAs, northern blot analyses of purifications done in one step (Figure 2B) or two steps (Figure 2C) were made. We were able to selectively isolate snR30 snoRNA in a one-step purification using streptavidin beads (Figure 2B). However, we realized that this one-step method brought many non-specific proteins (data not shown). Severe protein contamination in single-step purification protocols with RNA tags is not uncommon (38). To minimize protein contamination, we first enriched the

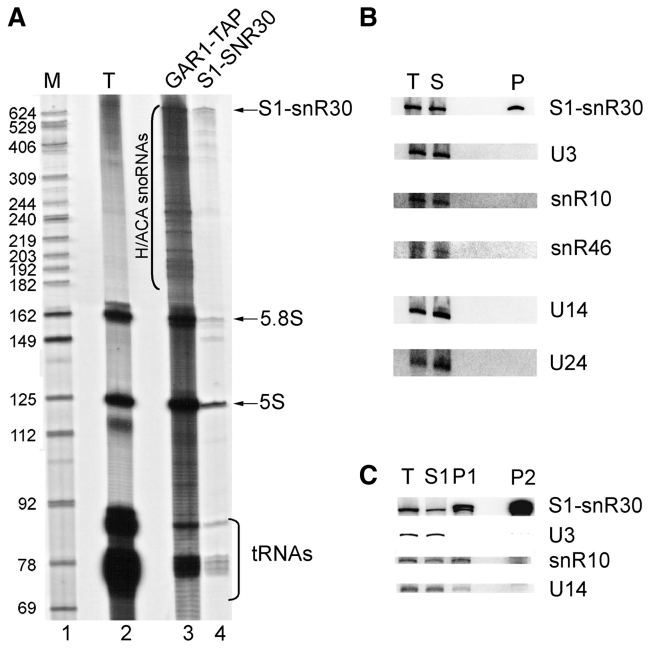


**Figure 2.** Selective purification of S1-tagged snR30 snoRNP. One-step (A and B) or two-step (C) purifications were done with extracts prepared from the S1-SNR30 strain grown in YPD. (**A**) 3′-End labeling analysis of recovered RNAs. Labeled RNAs from the extract (T), Gar1-TAP IP and S1-snR30 purification were analyzed. Radiolabeled DNA markers (M) were run in parallel. S1-snR30, H/ACA snoRNAs, 5.8S and 5S rRNAs, and tRNAs are indicated. (**B**) Northern blots of RNAs recovered from one-step purification: extract (T), streptavidin flow through (S) and eluate (P). (**C**) Northern blots of RNAs recovered from two-step purification: extract (T), IgG flow through (S1), IgG eluate (P1) and streptavidin eluate (P2). For B and C, snoRNAs analyzed are indicated on the right of each panel.

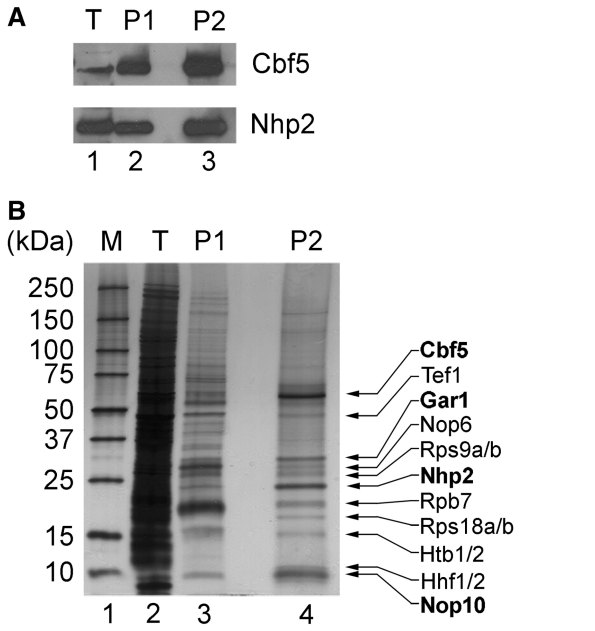


**Figure 3.** Purified S1-snR30 contains H/ACA proteins and a number of additional proteins. Proteins present in the extract (T), IgG eluate (P1) and streptavidin eluate (P2) were separated by SDS–PAGE and subjected to immunoblotting to detect Cbf5 and Nhp2 (**A**). In (**B**), the Criterion XT gel was silver-stained. Proteins identified by MS are indicated on the right. The molecular weights of protein markers (lane 1) are indicated on the left in kDa.

sample in H/ACA snoRNPs through Gar1-TAP purification, and then used the S1 aptamer in a second round of purification. Fewer proteins were detected with the two-step purification procedure. Importantly, we were able to specifically recover the snR30 snoRNA (Figure 2C). Note that in Figure 2C, the fuzzy signal seen in lane P2 of the snR10 panel comes from slight degradation of the abundant S1-snR30.

Co-purified proteins isolated in the two-step procedure were analyzed by western blotting. Detection of Cbf5 and Nhp2 indicated that recovered snR30 RNA was associated with H/ACA proteins (Figure 3A). Proteins fractionated by PAGE were also visualized by silver staining, and the dominant bands were subjected to MS analysis. As expected, MS results revealed that proteins Cbf5, Gar1, Nhp2 and Nop10 were highly enriched in purified samples (these proteins are indicated in bold in Figure 3B). The presence of the four H/ACA proteins demonstrated that the S1 aptamer did not interfere with their association with snR30 snoRNA, consistent with the observation that S1-tagged snR30 snoRNP is fully functional (Figure 1). No proteins of C/D snoRNPs or ribosomal proteins of the large subunit were recovered, indicating that the purification procedure was highly specific for snR30 RNP. A number of additional proteins not previously known to be associated with snR30 RNP were also identified by MS analysis: Nop6, translation elongation factor Tef1, RNA polymerase II subunit Rpb7, small ribosomal subunit proteins S9 and S18, and histones H2B and H4 (Figure 3B).

### Association of TAP-tagged proteins Nop6, Rps9A/B, Rps18A/B, Htb1/2 and Hhf2 with snR30 snoRNA

To validate the MS results, we carried out IPs with TAP-tagged versions of each protein and analyzed the co-precipitated RNAs by northern hybridization. MS analyses could not discriminate between the two isoforms of ribosomal proteins S9 (Rps9A and Rps9B) and S18 (Rps18A and Rps18B), as well as histones H2B (Htb1 and Htb2) and H4 (Hhf1 and Hhf2). Therefore, we carried out IPs with each isoform of these proteins. The efficiency of IPs was evaluated by western blot analysis (Supplementary Figure S1). The IPs confirmed that, like the H/ACA proteins, proteins Nop6, Rps9A/B, Rps18A/B, Htb1/2 and Hhf2 are associated with snR30 snoRNA *in vivo* (Figure 4). Only trace amounts of snR30 RNA were detected in control IPs with extracts from the untagged wild-type strain (Figure 4, BY4741 lanes). Nop6, ribosomal proteins S9 and S18, and histones Htb1, Htb2 and Hhf2 are not specific to snR30 since other snoRNAs were co-immunoprecipitated; it is also important to underscore that these proteins do not co-immunoprecipitate the same set of snoRNAs. None of the snoRNAs analyzed by northern hybridization co-immunoprecipitated with TAP-tagged proteins Rpb7 and Tef1, indicating that they were non-specific contaminants recovered during purification of snR30 snoRNP.

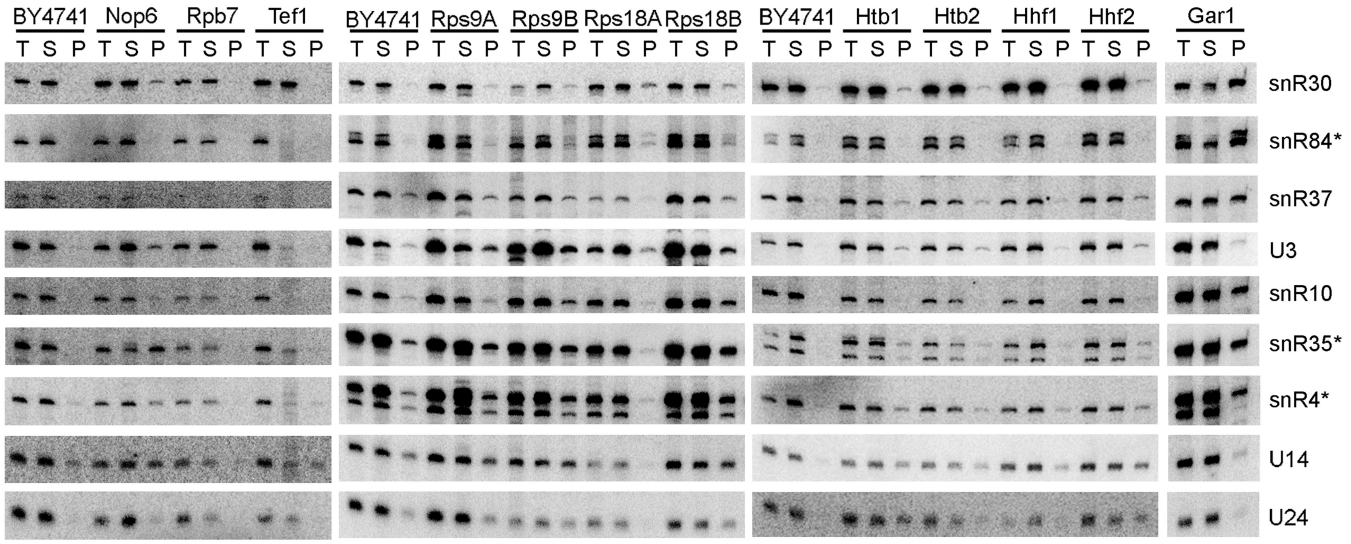


**Figure 4.** Analysis of snoRNAs that co-immunoprecipitate with TAP-tagged proteins. RNAs from total extract (T; 1% input), supernatant (S; 1%) and immunoprecipitates (P; 100%; Gar1-TAP 20%) were detected by northern hybridization. TAP-tagged proteins are identified at the top. Untagged BY4741 strain was used to determine background levels of immunoprecipitated snoRNAs, which are indicated on the right of each panel. The asterisk indicates blots with multiple bands: snR84 is the bottom band, snR35 is the top band, and snR4 is the bottom band.

Contamination of purified RNPs with Tef1 is well documented (39). For Nop6 IPs, snoRNAs U3, U14, snR4 and snR35 were also detected in addition to snR30; surprisingly, snR35 was the most enriched snoRNA of those tested.

### Endogenous Nop6 localizes to the nucleolus and cosediments with snR30 snoRNP in sucrose gradients

One of the novel proteins associated with snR30 snoRNP is Nop6, a protein bearing a predicted RNA recognition motif and a putative coiled-coil motif (our unpublished observations). Little is known about Nop6, though bioinformatics analyses implied that it functions in rRNA processing (40), and large-scale purification analyses indicated that it interacts with Gar1, Cbf5 and Nhp2, three of the four H/ACA proteins (41–43). These features make Nop6 a perfect candidate to associate with the snR30 RNP. A previous high-throughput study by Huh *et al.* (44) showed that GFP-tagged Nop6 localized to the nucleolus; however, these authors carefully cautioned that fusion to GFP could cause mislocalization of fusion proteins. We used anti-Nop6 antibodies to determine the cellular localization of endogenous Nop6 by immunofluorescence microscopy and showed that it co-localizes with the nucleolar protein Nop1 (Figure 5). We also investigated whether the depletion of snR30 snoRNA would alter the nucleolar localization of Nop6. Although Nop6 slightly stained the nucleoplasm of snR30-depleted cells ($t = 12$), the bulk of Nop6 remained in the nucleolus (Figure 5).

We analyzed the sedimentation profiles of Nop6 and snR30 snoRNA in sucrose density gradients. In addition, we asked whether the absence of snR30 would affect the sedimentation profile of Nop6, and vice versa. Figure 6A shows the sedimentation profile of snR30 RNA in various strains. In the GAR1-TAP strain and the

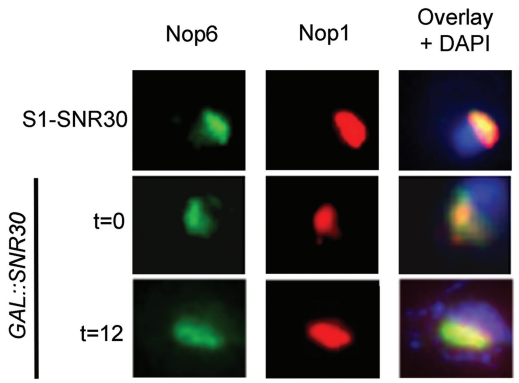


**Figure 5.** Nop6 localizes to the nucleolus in normal and snR30 snoRNA-depleted cells. S1-SNR30 cells grown in YPD, and *GAL::SNR30* cells grown in YPGal ($t = 0$) and YPD for 12 h ($t = 12$) were fixed and immunostained with purified anti-Nop6 antibodies (green) and anti-fibrillarin (Nop1) monoclonal antibody (red). The overlay is shown with the DAPI staining.

*GAL::SNR30* strain (grown in YPGal), snR30 snoRNA is most highly concentrated in low-density fractions, corresponding to a sedimentation coefficient of about 40S (Figure 6A). With strain *GAL::SNR30* larger amounts of snR30 RNA are seen in fractions 4 through 8; this modified sedimentation pattern could result from the high expression levels of snR30 snoRNA, which is under the control of the strong GAL1 promoter. When transcription of snR30 was turned off for 12 h [strain *GAL::SNR30* ($t = 12$) in YPD], the remaining snR30 snoRNA accumulated in the ~40S fraction and fraction 16, which corresponds to complexes that are larger than polysomes. When Nop6 was absent (profile with deletion strain *nop6*Δ in Figure 6A), a somewhat larger proportion of snR30 snoRNP was detected in complexes larger than

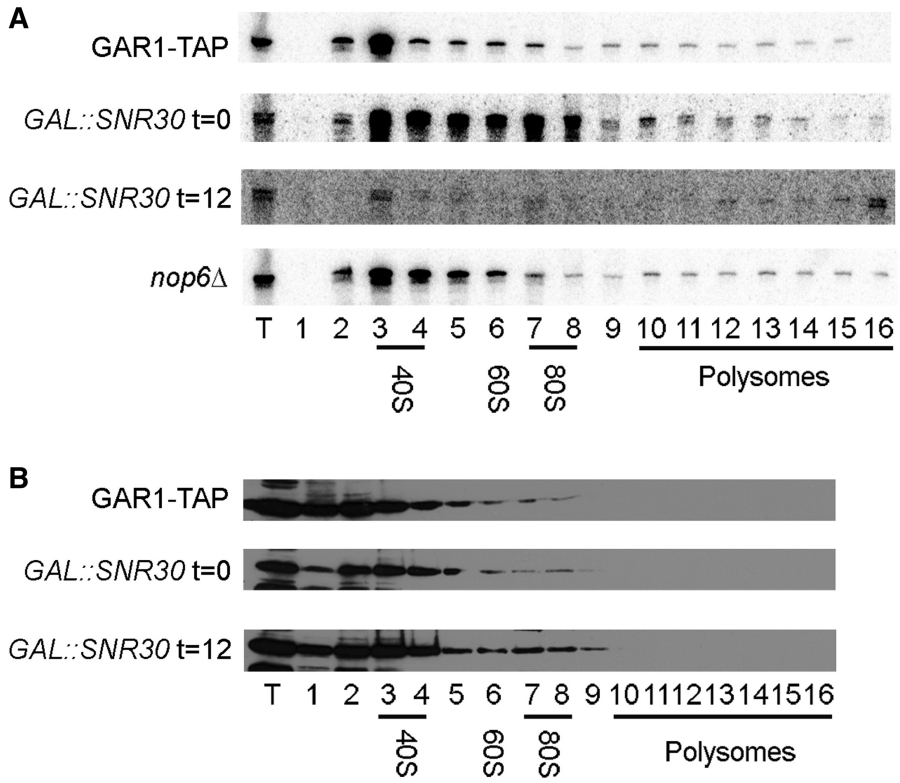


**Figure 6.** Sucrose gradient sedimentation analyses. Cellular extracts prepared from strains GAR1-TAP, *GAL::SNR30* either undepleted ($t = 0$) or depleted for 12 h ($t = 12$), and *nop6Δ* were fractionated on sucrose gradients. Total extract (T) and gradient fractions (1–16) are indicated. The positions of 40S and 60S ribosomal subunits, 80S ribosomes, and polysomes are indicated, based on the continuous $A_{254}$ absorbance profile. Northern blotting (**A**) was done with a $^{32}$P-labeled oligonucleotide complementary to snR30 snoRNA. (**B**) Western blots of corresponding gradients were carried out with anti-Nop6 antibodies.

40S as compared to control cells, with a gradual trailing of snR30 RNA towards fractions 4, 5 and 6. This profile is distinct from that seen for snR30 RNA in control strain GAR1-TAP.

The sedimentation profile of Nop6 was also analyzed in the presence and absence of snR30 RNA (Figure 6B). In the GAR1-TAP and *GAL::SNR30* strains, Nop6 co-sedimented with snR30 snoRNP in low-density fractions. Depletion of snR30 snoRNA did not affect the sedimentation profile of Nop6, which was still found in low-density fractions (Figure 6B). Taken together, these results suggest that Nop6 does not require snR30 snoRNP to sediment with complexes of ~40S, but the absence of Nop6 slightly alters the sedimentation profile of snR30 snoRNP.

To determine if the absence of snR30 snoRNA has an impact on Nop6 association with other snoRNAs, Nop6-TAP IPs were carried out before ($t = 0$) and after ($t = 12$) depletion of snR30 RNA (Figure 7). In cells depleted of snR30 snoRNA the association of Nop6 with snoRNAs U3, U14, snR4 and snR35 was disrupted (Figure 7).

### The snR30 snoRNA is required for cleavage at sites A0, A1 and A2, and absence of Nop6 affects cleavage at site A2

Cleavage of pre-rRNA at site A0 is dispensable for growth (9). Atzorn *et al.* (15) reported that snR30 snoRNP is involved in cleavages at sites A0, A1 and A2 but this was based on northern blot results from Morrissey and Tollervey (19). Using the primer extension method, which is a more precise approach because the exact position of any break/cleavage can be mapped, we demonstrate that snR30 snoRNP is required for cleavages at sites A0, A1 and A2. Wild-type strain YPH499 was used as a positive control for cleavages; primer extension stops can be observed at the 5′-end of the pre-rRNA and at the A0, A1 and A2 cleavage sites (Figure 8). When cells were depleted of snR30 snoRNA, there was a complete loss of the primer extension signal corresponding to site A0 and A2 cleavages (Figure 8A and C). Since the A1 cleavage site corresponds to the 5′-end of mature 18S rRNA, which is still abundant even after a 12-h depletion of snR30 RNA, we could not see variations in the primer extension signal corresponding to site A1 when using the 18S probe (Figure 8B). However, the signal for the 5′-end is slightly stronger when snR30 RNA is depleted, suggesting that there is accumulation of pre-rRNA that is not cleaved at site A1. Since Nop6 is not an essential protein, we wanted to determine if it could be implicated in site A0 cleavage, which is dispensable for growth (9). Primer extension experiments with RNAs isolated from strain *nop6Δ* generated similar results to the wild-type strain YPH499 for cleavages at sites A0 and A1, indicating that Nop6 is not required for these cleavages. Interestingly, a slight decrease in primer extension stop

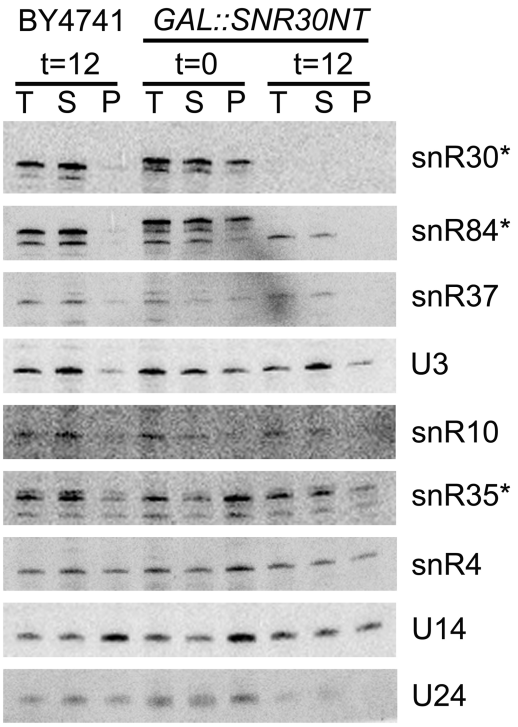


**Figure 7.** Depletion of snR30 snoRNA disrupts Nop6 association with other snoRNAs. Shown are RNAs immunoprecipitated with Nop6-TAP. RNAs from total extract (T; 1% input), supernatant (S; 1%) and immunoprecipitates (P) were detected by northern hybridization. Strains and time of growth in YPD are indicated at the top. Untagged BY4741 strain was used to determine background levels of immunoprecipitated snoRNAs, which are indicated on the right of each panel. The asterisk indicates blots with multiple bands: snR30 is the top band, snR84 is the bottom band, snR35 is the top band.

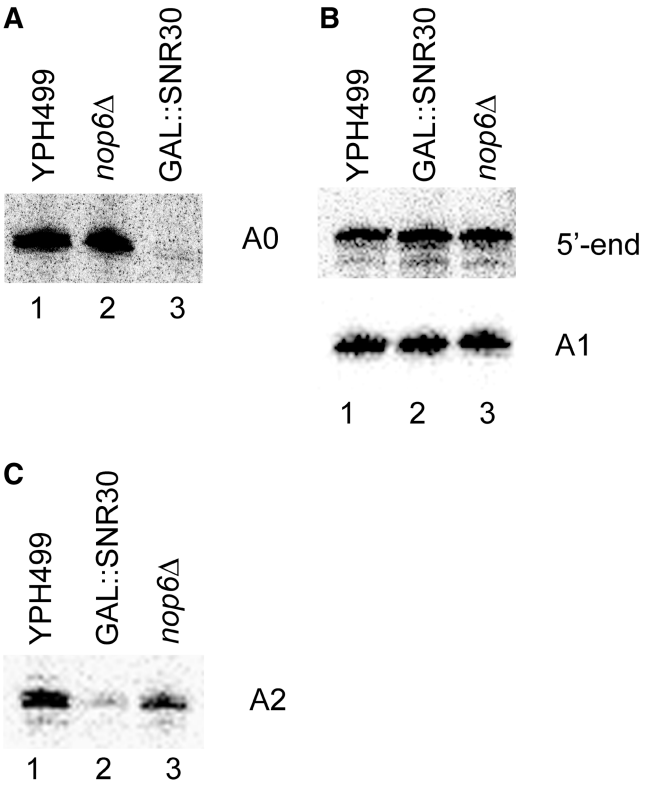


**Figure 8.** Analysis of pre-rRNA processing at sites A0, A1 and A2. Total RNA used for primer extension was extracted from wild-type strain YPH499, strain *nop6*Δ or strain *GAL::SNR30* grown for 12 h in YPD. The primers hybridize downstream of the A0 site (**A**), near the 5′-end of mature 18S rRNA (**B**) and between A2 and A3 sites (**C**). The position of the primer extension stops at the 5′-end of the pre-rRNA or as a result of the cleavages is indicated.

at site A2 was observed with RNAs isolated from the *nop6*Δ strain (compare lanes 1 and 3 in Figure 8C).

### Absence of snR30 snoRNP impairs mature SSU processome assembly

We carried out EM analyses of chromatin spreads prepared from cells of *GAL::SNR30* strain grown in YPGal and cells grown for 5 h in YPD to deplete snR30 snoRNA (Figure 9). Depletion of snR30 RNA appeared to have little effect on rRNA transcription based on the high density of transcripts on many rRNA genes (Figure 9B) similar to non-depleted cells (Figure 9A). However, normal co-transcriptional rRNA processing events were impaired in snR30-depleted cells. Specifically, formation of SSU processomes and cleavage of nascent transcripts (thought to be at site A2) did not occur after snR30 snoRNA depletion, although both occurred as expected (12,14) in non-depleted cells. (Compare the blowups of transcripts at the 3′-end of genes in Figure 9A and B, with cleaved transcripts seen in 9A and uncleaved transcripts seen in 9B).

## DISCUSSION

The H/ACA snoRNA snR30 has no known pseudouridylation target but it is essential for the early processing events that lead to 18S rRNA production. The mechanism by which snR30 snoRNP participates in these cleavage reactions is still a mystery. Identifying the protein components of snR30 snoRNP could give us insights into its function in pre-rRNA processing reactions. With the two-step purification procedure that we designed (purification of H/ACA snoRNPs through Gar1-TAP in the first step, followed by selective isolation of S1-tagged snR30), we were able to recover the snR30 RNA, the four H/ACA proteins and eight novel proteins: Nop6, Rps9A/B, Rsp18A/B, Htb1/2 and Hhf2. The snR30 snoRNP was purified previously by the Lührmann group (16), who carried out an anti-TMG immunoaffinity chromatography to enrich the samples in TMG-capped RNPs followed by U1 snRNP depletion and Mono Q anion-exchange chromatography; they identified seven snR30-associated proteins with apparent molecular masses of **65**, 48, 46, 38, **25**, **23**, **10** kDa, four of which (in bold) were later identified as H/ACA proteins (18). Because other snoRNAs as well as snRNAs were detected in the purified samples, it remained unclear whether proteins of 48, 46 and 38 kDa were genuine snR30-associated proteins. Lübben *et al.* (16) even suggested that the 38-kDa protein might be Nop1, a common protein of the C/D snoRNPs. The Lührmann group subsequently used the same purification scheme in

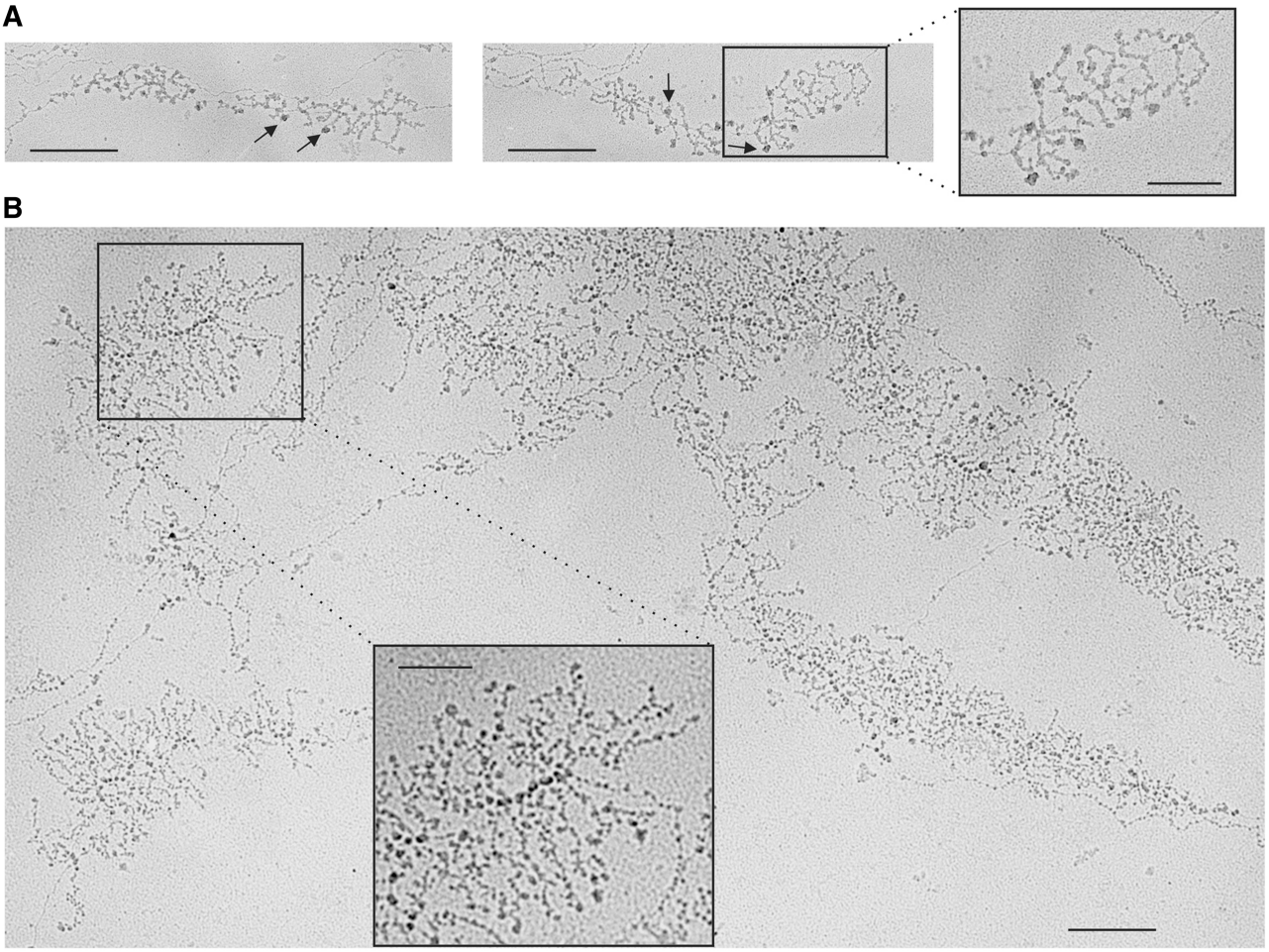


**Figure 9.** EM analysis of chromatin spreads from yeast strain *GAL::SNR30*. The strain was grown in YPGal (**A**; non-depleted) and shifted to YPD for 5 h to deplete cells of snR30 snoRNA (**B**). Examples of two representative rRNA genes from non-depleted cells are shown in (A), while (B) shows an overview of several active rRNA genes from depleted cells, at the same magnification as genes in (A). Scale bars = 0.4 μm. Arrows in (A) indicate SSU processomes. In both (A) and (B), a blowup is shown of the 3′-end of a gene (both at the same magnification and both demarcated by black boxes). Scale bars in blowups = 0.2 μm.

order to identify snR30 proteins via mass spectrometry (18); the four common H/ACA proteins and Sm proteins were identified, but not the previously isolated proteins of 48, 46 and 38 kDa; it is therefore possible that these three proteins are not snR30-associated. A more recent affinity purification of the snR30 snoRNP by Liang and Fournier (45) showed that it was associated with DEAD-box RNA helicase Has1. To purify snR30 snoRNP, these authors inserted the human U1 hairpin II sequence in the snR30 snoRNA, and the construct was expressed in a strain that also expressed the HA-tagged UA1 protein, which specifically binds to U1 hairpin II. We did not find Has1 in our preparations of purified snR30 RNP. This could be due to the purification method, which was different from that of Liang and Fournier (45). It is also possible that the site where the S1 aptamer was inserted in snR30 snoRNA could interfere with Has1 binding. In any case, it is known that Has1 is not an snR30-specific protein because it was strongly associated with U3, U14 and snR63 snoRNAs, and with U1 and U6 snRNAs (45). Similarly, DEAD-box RNA helicase Rok1 was shown to be specifically required for the release of snR30 snoRNP from pre-ribosomal particles (46) but Rok1 was not found in our purified complexes. This could also be explained by the transient nature of the interactions between RNA helicases and RNA.

We found that Nop6 can associate with snR30 snoRNP. Nop6 has many features that make it a perfect candidate to function with the snR30 RNP: it contains putative RRM and coiled-coil motifs (our unpublished observations), it localizes to the nucleolus (44), it is associated with H/ACA proteins (41–43) and it is implicated in 40S ribosomal subunit biogenesis (47). Nop6 could bind directly to snR30 snoRNA through its RRM or to the RNP via protein–protein interactions using its coiled-coil motif. However, Nop6 is not an snR30-specific protein. In fact, we found that Nop6 interacts more strongly with snR35 H/ACA snoRNA (Figure 4). This is interesting when considered in view of recent work by Buchhaupt *et al.* (48) who found that mutations in Nop6 can suppress malfunction of Nep1, an N1-specific pseudouridine methyltransferase that

modifies Ψ1191 of 18S rRNA (49). The H/ACA snoRNA snR35 mediates isomerisation of U1191 into Ψ1191, which is required for proper D-site cleavage (50). Although Nop6 is not essential for yeast growth, the absence of Nop6 reduces the efficiency of cleavage at site A2 [Figure 8C and (47)]. Lack of Nop6 could have discrete effects on rRNA structure near U/Ψ1191, which in turn could hinder proper A2 cleavage. These structural changes could affect the levels of mature rRNA but not to a point where an effect on growth could be observed (47). Alteration of 18S rRNA structure triggered by the absence of Nop6 could explain why a knock-out of Nep1 is tolerated in the mutant strain (48). Interestingly, Nop6 interaction with snR35 and other snoRNAs was disrupted in snR30-depleted cells (Figure 7) but Nop6 still sedimented with complexes of ~40S. Lack of snR30 could prevent structural changes in 18S rRNA, thus inhibiting the binding of certain snoRNAs but not binding of Nop6.

Ribosomal proteins Rps9 and Rps18, which are conserved from bacteria to humans, were found in association with snR30 RNA. This suggests that they might have extraribosomal roles (51,52) in rRNA biogenesis and processing, as has been demonstrated for Rps19 and Rps24 (53,54). Indeed, Rps9 was previously identified as a stable component of the SSU processome together with a few other ribosomal proteins (such as Rps4, Rps6, Rps7, and Rps14) thus implicating these proteins in cleavages A0, A1 and A2 (11,55). Similarly, Rps9 and Rps18 could have processing functions when associated with snR30 snoRNP. In yeast, Rps9 and Rps18 are expressed from duplicated genes. Rps9A and Rps9B are 97% identical, while Rps18A and Rps18B have identical amino acid sequences. Our results show that levels of snR30 snoRNA associated with Rps9A and Rps9B are similar (Figure 4). However, Rps18A was more strongly associated with snR30 snoRNA than Rps18B. It was shown by Komili *et al*. (56) that there are differences between the functional roles of ribosomal protein paralogs when cells are lacking specific ribosomal proteins. More specifically, loss of proteins Loc1 or Puf6, which are implicated in ribosomal assembly, caused paralog-specific localization defects of GFP-tagged ribosomal proteins. For example, Rps18B localizes to a region consistent with the endoplasmic reticulum in *loc1*Δ cells, while Rps18A exhibits wild-type localization. We found that Rps9A and Rps9B do not bind the same population of snoRNAs, and this is also the case for Rps18A and Rps18B (Figure 4). These results support the view that Rps9 and Rps18 duplicates could have different roles in ribosome biogenesis and function. Differences in expression levels or in spatio-temporal expression of the identical ribosomal proteins S18A and S18B could account for their functional differences.

As mentioned above, Rps9 has been identified as a stable component of the SSU processome (55). Here we showed that Rps9 can co-immunoprecipitate other snoRNAs, implying that the SSU processome could contain not only the U3 snoRNP and pre-rRNA, but also a subset of processing and modifying snoRNPs. In support of this idea, we have demonstrated that snR30 snoRNA is required for the formation of the SSU processome, which is seen by EM at the 5′-end of nascent pre-rRNA transcripts (Figure 9). Thus, the role of snR30 snoRNP in pre-rRNA processing could be directly linked to the formation of these large terminal knobs since they are required for pre-rRNA processing reactions, including cleavage at sites A0, A1 and A2 (11,12). No or only small 5′-end RNP particles can be observed when snR30 RNA is depleted, suggesting that the role of snR30 snoRNP might be to stabilize U3 snoRNP binding to nascent pre-rRNA and/or to chaperone the assembly steps and structural rearrangements that result in SSU processome formation. Our results are consistent with the recent identification of the snR30 snoRNA-binding site within 18S rRNA (20) in a region that becomes compacted into the SSU processome (12).

We also found that snR30 snoRNP is associated with histones H2B (Htb1 and Htb2) and H4 (Hhf2). It has been shown that histones H3 and H4 do not negatively regulate transcription but are rather associated with actively transcribed rRNA genes; indeed, they are components of the upstream activating factor (UAF), a transcription factor required for RNA polymerase I transcription in *S. cerevisiae* (57). It is possible that snR30 snoRNP could act as a chaperone, linking rRNA transcription and processing at early stages of rRNA transcription. Interaction of snR30 snoRNP with histones could mediate its recruitment to the nascent SSU processome, facilitating co-transcriptional cleavage of the pre-rRNA at sites A0, A1 and A2.

A general feature of IPs with TAP-tagged proteins was that the signal for snR30 snoRNA was weak, although consistently above background levels seen in control IPs made with extracts prepared from the untagged strain BY4741. Similar results have been observed with ribosomal proteins that associate with the U3 snoRNA (55). Since most ribosomal proteins are constituents of cytoplasmic ribosomes, only a tiny fraction of these proteins could be implicated in pre-rRNA processing and maturation. Similarly, most histones are associated with non-ribosomal DNA, leaving only few histone molecules associated with rDNA and snR30 snoRNP. It is also possible that the low levels of snR30 RNA co-immunoprecipitated with Nop6, ribosomal proteins and histones could reflect transient association between these molecules. In any case, the identified proteins are clearly associated with snR30 snoRNA, but like the common H/ACA proteins, they are not snR30-specific. Furthermore, these proteins co-immunoprecipitated different subsets of snoRNAs; this is possibly a consequence of the order of assembly/maturation events that are required for optimal ribosome biogenesis.

The major aim of this work was to identify the protein content of snR30 snoRNP since the identification of such proteins could help us understand how this RNP participates in early pre-rRNA processing events. We have identified novel proteins that associate with snR30 and other snoRNAs. Notably, all these proteins co-immunoprecipitated the U3 snoRNA, which suggests they could be part of the SSU processome (58). Considering that snR30 RNA associates with these

proteins and the fact that it is required for SSU processome assembly but does not co-sediment with the SSU processome in sucrose density gradients, we propose that snR30 is a transiently associated SSU processome factor. Overall, our findings give insights into snR30's function, and how it could link rRNA transcription and processing via its role in SSU processome assembly and its interaction with ribosomal proteins and histones.

## SUPPLEMENTARY DATA

Supplementary Data are available at NAR Online.

## ACKNOWLEDGEMENTS

The authors are very grateful to David Engelke (University of Michigan), Yves Henry (Université de Toulouse), Michael Pollard (The Scripps Research Institute) and Bernard Turcotte (McGill University) for reagents and advice, and to Jesús de la Cruz (Universidad de Sevilla) for critical reading of the article and communicating data prior to publication. The authors also thank Krasimir Spasov, Catherine Payant and Martin Lapansée for technical assistance.

## FUNDING

Fonds québécois de la recherche sur la nature et les technologies (FQRNT) PhD studentship (to V.L.); FQRNT (NC-80168); Fonds de la recherche en santé du Québec (FRSQ; NC-2843); Canadian Institutes of Health Research (MOP-64290); National Sciences and Engineering Research Council of Canada (NSERC; RGPIN/249792-2009) (to F.D); National Science Foundation (MCB-0818818) (to A.L.B.); Chercheur-boursier award of the FRSQ (to F.D.). Funding for open access charge: NSERC.

*Conflict of interest statement*. None declared.

## REFERENCES

1. Kressler,D., Hurt,E. and Bassler,J. (2010) Driving ribosome assembly. *Biochim. Biophys. Acta*, **1803**, 673–683.
2. Reichow,S.L., Hamma,T., Ferré-D'Amaré,A.R. and Varani,G. (2007) The structure and function of small nucleolar ribonucleoproteins. *Nucleic Acids Res.*, **35**, 1452–1464.
3. Piekna-Przybylska,D., Decatur,W.A. and Fournier,M.J. (2007) New bioinformatic tools for analysis of nucleotide modifications in eukaryotic rRNA. *RNA*, **13**, 305–312.
4. Ni,J., Tien,A.L. and Fournier,M.J. (1997) Small nucleolar RNAs direct site-specific synthesis of pseudouridine in ribosomal RNA. *Cell*, **89**, 565–573.
5. Ganot,P., Bortolin,M.L. and Kiss,T. (1997) Site-specific pseudouridine formation in preribosomal RNA is guided by small nucleolar RNAs. *Cell*, **89**, 799–809.
6. Balakin,A.G., Smith,L. and Fournier,M.J. (1996) The RNA world of the nucleolus: two major families of small RNAs defined by different box elements with related functions. *Cell*, **86**, 823–834.
7. Ganot,P., Caizergues-Ferrer,M. and Kiss,T. (1997) The family of box ACA small nucleolar RNAs is defined by an evolutionarily conserved secondary structure and ubiquitous sequence elements essential for RNA accumulation. *Genes Dev.*, **11**, 941–956.
8. Darzacq,X., Kittur,N., Roy,S., Shav-Tal,Y., Singer,R.H. and Meier,U.T. (2006) Stepwise RNP assembly at the site of H/ACA RNA transcription in human cells. *J. Cell. Biol.*, **173**, 207–218.
9. Venema,J. and Tollervey,D. (1999) Ribosome synthesis in *Saccharomyces cerevisiae*. *Annu Rev Genet*, **33**, 261–311.
10. Lygerou,Z., Allmang,C., Tollervey,D. and Séraphin,B. (1996) Accurate processing of a eukaryotic precursor ribosomal RNA by ribonuclease MRP in vitro. *Science*, **272**, 268–270.
11. Dragon,F., Gallagher,J.E., Compagnone-Post,P.A., Mitchell,B.M., Porwancher,K.A., Wehner,K.A., Wormsley,S., Settlage,R.E., Shabanowitz,J., Osheim,Y. *et al.* (2002) A large nucleolar U3 ribonucleoprotein required for 18S ribosomal RNA biogenesis. *Nature*, **417**, 967–970.
12. Osheim,Y.N., French,S.L., Keck,K.M., Champion,E.A., Spasov,K., Dragon,F., Baserga,S.J. and Beyer,A.L. (2004) Pre-18S ribosomal RNA is structurally compacted into the SSU processome prior to being cleaved from nascent transcripts in *Saccharomyces cerevisiae*. *Mol. Cell*, **16**, 943–954.
13. Grandi,P., Rybin,V., Bassler,J., Petfalski,E., Strauss,D., Marzioch,M., Schäfer,T., Kuster,B., Tschochner,H., Tollervey,D. *et al.* (2002) 90S pre-ribosomes include the 35S pre-rRNA, the U3 snoRNP, and 40S subunit processing factors but predominantly lack 60S synthesis factors. *Mol. Cell*, **10**, 105–115.
14. Kos,M. and Tollervey,D. (2010) Yeast pre-rRNA processing and modification occur cotranscriptionally. *Mol. Cell*, **37**, 809–820.
15. Atzorn,V., Fragapane,P. and Kiss,T. (2004) U17/snR30 is a ubiquitous snoRNA with two conserved sequence motifs essential for 18S rRNA production. *Mol. Cell Biol.*, **24**, 1769–1778.
16. Lübben,B., Fabrizio,P., Kastner,B. and Lührmann,R. (1995) Isolation and characterization of the small nucleolar ribonucleoprotein particle snR30 from *Saccharomyces cerevisiae*. *J. Biol. Chem.*, **270**, 11549–11554.
17. Henras,A., Henry,Y., Bousquet-Antonelli,C., Noaillac-Depeyre,J., Gélugne,J.-P. and Caizergues-Ferrer,M. (1998) Nhp2p and Nop10p are essential for the function of H/ACA snoRNPs. *EMBO J.*, **17**, 7078–7090.
18. Watkins,N.J., Gottschalk,A., Neubauer,G., Kastner,B., Fabrizio,P., Mann,M. and Lührmann,R. (1998) Cbf5p, a potential pseudouridine synthase, and Nhp2p, a putative RNA-binding protein, are present together with Gar1p in all H BOX/ACA-motif snoRNPs and constitute a common bipartite structure. *RNA*, **4**, 1549–1568.
19. Morrissey,J.P. and Tollervey,D. (1993) Yeast snR30 is a small nucleolar RNA required for 18S rRNA synthesis. *Mol. Cell Biol.*, **13**, 2469–2477.
20. Fayet-Lebaron,E., Atzorn,V., Henry,Y. and Kiss,T. (2009) 18S rRNA processing requires base pairings of snR30 H/ACA snoRNA to eukaryote-specific 18S sequences. *EMBO J.*, **28**, 1260–1270.
21. Taylor,D.J., Devkota,B., Huang,A.D., Topf,M., Narayanan,E., Sali,A., Harvey,S.C. and Frank,J. (2009) Comprehensive molecular structure of the eukaryotic ribosome. *Structure*, **17**, 1591–1604.
22. Bally,M., Hughes,J. and Cesareni,G. (1988) SnR30: a new, essential small nuclear RNA from *Saccharomyces cerevisiae*. *Nucleic Acids Res.*, **16**, 5291–5303.
23. Ausubel,F.M., Brent,R., Kingston,R.E., Moore,D.D., Seidman,J.G., Smith,J.A. and Struhl,K. (eds), (1999) *Short Protocols in Molecular Biology: A Compendium of Methods from Current Protocols in Molecular Biology*, 4th edn. John Wiley & Sons, New York.
24. Srisawat,C. and Engelke,D.R. (2001) Streptavidin aptamers: affinity tags for the study of RNAs and ribonucleoproteins. *RNA*, **7**, 632–641.
25. Higuchi,R., Krummel,B. and Saiki,R.K. (1988) A general method of in vitro preparation and specific mutagenesis of DNA fragments: study of protein and DNA interactions. *Nucleic Acids Res.*, **16**, 7351–7367.
26. Sikorski,R.S. and Hieter,P. (1989) A system of shuttle vectors and yeast host strains designed for efficient manipulation of DNA in *Saccharomyces cerevisiae*. *Genetics*, **122**, 19–27.
27. Gietz,D., St Jean,A., Woods,R.A. and Schiestl,R.H. (1992) Improved method for high efficiency transformation of intact yeast cells. *Nucleic Acids Res.*, **20**, 1425.

28. Rigaut,G., Shevchenko,A., Rutz,B., Wilm,M., Mann,M. and Séraphin,B. (1999) A generic protein purification method for protein complex characterization and proteome exploration. *Nat. Biotechnol.*, **17**, 1030–1032.
29. Longtine,M.S., McKenzie,A. 3rd, Demarini,D.J., Shah,N.G., Wach,A., Brachat,A., Philippsen,P. and Pringle,J.R. (1998) Additional modules for versatile and economical PCR-based gene deletion and modification in *Saccharomyces cerevisiae*. *Yeast*, **14**, 953–961.
30. Dragon,F., Pogacic,V. and Filipowicz,W. (2000) In vitro assembly of human H/ACA small nucleolar RNPs reveals unique features of U17 and telomerase RNAs. *Mol. Cell Biol.*, **20**, 3037–3048.
31. Venema,J., Planta,R.J. and Raué,H.A. (1998) *In vivo* mutational analysis of ribosomal RNA in *Saccharomyces cerevisiae*. *Methods Mol. Biol.*, **77**, 257–270.
32. Henras,A., Dez,C., Noaillac-Depeyre,J., Henry,Y. and Caizergues-Ferrer,M. (2001) Accumulation of H/ACA snoRNPs depends on the integrity of the conserved central domain of the RNA-binding protein Nhp2p. *Nucleic Acids Res.*, **29**, 2733–2746.
33. Nesterenko,M.V., Tilley,M. and Upton,S.J. (1994) A simple modification of Blum's silver stain method allows for 30 minute detection of proteins in polyacrylamide gels. *J. Biochem. Biophys. Methods*, **28**, 239–242.
34. Kressler,D., de la Cruz,J., Rojo,M. and Linder,P. (1997) Fal1p is an essential DEAD-box protein involved in 40S-ribosomal-subunit biogenesis in *Saccharomyces cerevisiae*. *Mol. Cell. Biol.*, **17**, 7283–7294.
35. Pringle,J.R., Preston,R.A., Adams,A.E., Stearns,T., Drubin,D.G., Haarer,B.K. and Jones,E.W. (1989) Fluorescence microscopy methods for yeast. *Methods Cell Biol.*, **31**, 357–435.
36. Yang,J.M., Baserga,S.J., Turley,S.J. and Pollard,K.M. (2001) Fibrillarin and other snoRNP proteins are targets of autoantibodies in xenobiotic-induced autoimmunity. *Clin. Immunol.*, **101**, 38–50.
37. Dunbar,D.A., Wormsley,S., Agentis,T.M. and Baserga,S.J. (1997) Mpp10p, a U3 small nucleolar ribonucleoprotein component required for pre-18S rRNA processing in yeast. *Mol. Cell. Biol.*, **17**, 5803–5812.
38. Hogg,J.R. and Collins,K. (2007) RNA-based affinity purification reveals 7SK RNPs with distinct composition and regulation. *RNA*, **13**, 868–880.
39. Oeffinger,M., Wei,K.E., Rogers,R., DeGrasse,J.A., Chait,B.T., Aitchison,J.D. and Rout,M.P. (2007) Comprehensive analysis of diverse ribonucleoprotein complexes. *Nat. Methods*, **4**, 951–956.
40. Samanta,M.P. and Liang,S. (2003) Predicting protein functions from redundancies in large-scale protein interaction networks. *Proc. Natl Acad. Sci. USA*, **100**, 12579–12583.
41. Ho,Y., Gruhler,A., Heilbut,A., Bader,G.D., Moore,L., Adams,S.L., Millar,A., Taylor,P., Bennett,K., Boutilier,K. *et al.* (2002) Systematic identification of protein complexes in *Saccharomyces cerevisiae* by mass spectrometry. *Nature*, **415**, 180–183.
42. Krogan,N.J., Cagney,G., Yu,H., Zhong,G., Guo,X., Ignatchenko,A., Li,J., Pu,S., Datta,N., Tikuisis,A.P. *et al.* (2006) Global landscape of protein complexes in the yeast Saccharomyces cerevisiae. *Nature*, **440**, 637–643.
43. Krogan,N.J., Peng,W.T., Cagney,G., Robinson,M.D., Haw,R., Zhong,G., Guo,X., Zhang,X., Canadien,V., Richards,D.P. *et al.* (2004) High-definition macromolecular composition of yeast RNA-processing complexes. *Mol. Cell*, **13**, 225–239.
44. Huh,W.K., Falvo,J.V., Gerke,L.C., Carroll,A.S., Howson,R.W., Weissman,J.S. and O'Shea,E.K. (2003) Global analysis of protein localization in budding yeast. *Nature*, **425**, 686–691.
45. Liang,X.H. and Fournier,M.J. (2006) The helicase Has1p is required for snoRNA release from pre-rRNA. *Mol. Cell. Biol.*, **26**, 7437–7450.
46. Bohnsack,M.T., Kos,M. and Tollervey,D. (2008) Quantitative analysis of snoRNA association with pre-ribosomes and release of snR30 by Rok1 helicase. *EMBO Rep.*, **9**, 1230–1236.
47. Garcia-Gomez,J.J., Babiano,R., Lebaron,S., Froment,C., Monsarrat,B., Henry,Y. and de la Cruz,J. (2011) Nop6, a component of 90S pre-ribosomal particles, is required for 40S ribosomal subunit biogenesis in *Saccharomyces cerevisiae*. *RNA Biol.*, **8**, 112–124.
48. Buchhaupt,M., Kotter,P. and Entian,K.D. (2007) Mutations in the nucleolar proteins Tma23 and Nop6 suppress the malfunction of the Nep1 protein. *FEMS Yeast Res.*, **7**, 771–781.
49. Wurm,J.P., Meyer,B., Bahr,U., Held,M., Frolow,O., Kotter,P., Engels,J.W., Heckel,A., Karas,M., Entian,K.D. *et al.* (2010) The ribosome assembly factor Nep1 responsible for Bowen-Conradi syndrome is a pseudouridine-N1-specific methyltransferase. *Nucleic Acids Res.*, **38**, 2387–2398.
50. Liang,X.H., Liu,Q. and Fournier,M.J. (2009) Loss of rRNA modifications in the decoding center of the ribosome impairs translation and strongly delays pre-rRNA processing. *RNA*, **15**, 1716–1728.
51. Wool,I.G. (1996) Extraribosomal functions of ribosomal proteins. *Trends Biochem. Sci.*, **21**, 164–165.
52. Warner,J.R. and McIntosh,K.B. (2009) How common are extraribosomal functions of ribosomal proteins? *Mol. Cell*, **34**, 3–11.
53. Léger-Silvestre,I., Caffrey,J.M., Dawaliby,R., Alvarez-Arias,D.A., Gas,N., Bertolone,S.J., Gleizes,P.E. and Ellis,S.R. (2005) Specific role for yeast homologs of the Diamond Blackfan anemia-associated Rps19 protein in ribosome synthesis. *J. Biol. Chem.*, **280**, 38177–38185.
54. Choesmel,V., Fribourg,S., Aguissa-Toure,A.H., Pinaud,N., Legrand,P., Gazda,H.T. and Gleizes,P.E. (2008) Mutation of ribosomal protein RPS24 in Diamond-Blackfan anemia results in a ribosome biogenesis disorder. *Hum. Mol. Genet.*, **17**, 1253–1263.
55. Bernstein,K.A., Gallagher,J.E., Mitchell,B.M., Granneman,S. and Baserga,S.J. (2004) The small-subunit processome is a ribosome assembly intermediate. *Eukaryot. Cell*, **3**, 1619–1626.
56. Komili,S., Farny,N.G., Roth,F.P. and Silver,P.A. (2007) Functional specificity among ribosomal proteins regulates gene expression. *Cell*, **131**, 557–571.
57. Tongaonkar,P., French,S.L., Oakes,M.L., Vu,L., Schneider,D.A., Beyer,A.L. and Nomura,M. (2005) Histones are required for transcription of yeast rRNA genes by RNA polymerase I. *Proc. Natl Acad. Sci. USA*, **102**, 10129–10134.
58. Phipps,K.R., Charette,J.M. and Baserga,S.J. (2011) The SSU processome in ribosome biogenesis - progress and prospects. *WIREs RNA*, **2**, 1–21.